

## Article

# The *Stegodon* Bonebed of the Middle Pleistocene Archaeological Site Mata Menge (Flores, Indonesia): Taphonomic Agents in Site Formation

Meagan J. Powley <sup>1,2,\*</sup>, Indra Sutisna <sup>3</sup>, Katarina M. Mikac <sup>2</sup>, Unggul Prasetyo Wibowo <sup>3</sup> and Gerrit D. van den Bergh <sup>1,\*</sup>

- <sup>1</sup> Centre for Archaeological Science, School of Earth, Atmospheric and Life Sciences, University of Wollongong, Wollongong, NSW 2522, Australia
- <sup>2</sup> Centre for Sustainable Ecosystem Solutions, School of Earth, Atmospheric and Life Sciences, University of Wollongong, Wollongong, NSW 2522, Australia; kmikac@uow.edu.au
- <sup>3</sup> Geology Museum Bandung, Geological Agency, Jalan Diponegoro 57, Bandung 40122, Indonesia; indra11084@yahoo.com (I.S.); uungpw@yahoo.com (U.P.W.)
- \* Correspondence: mjp94@uowmail.edu.au (M.J.P.); gert@uow.edu.au (G.D.v.d.B.)

**Abstract:** The Middle Pleistocene fluvial channel site of the Upper Fossil-bearing Interval at Mata Menge in the So'a Basin, Flores, Indonesia, has yielded the earliest fossil evidence for *Homo floresiensis* in association with stone artefacts and fossils of highly endemic insular fauna, including *Stegodon*, giant rats, crocodiles, Komodo dragons, and various birds. A preliminary taphonomic review of the fossil material here aimed to provide additional context for the hominin remains in this bonebed. Analysis was performed on two subsets of material from the same fluvial sandstone layer. Subset 1 comprised all material from two adjacent one-metre square quadrants ( $n = 91$ ), and Subset 2 all *Stegodon* long limb bones excavated from the same layer ( $n = 17$ ). Key analytical parameters included species and skeletal element identification; fossil size measurements and fragmentation; weathering stages; bone fracture characteristics; and other biological and geological bone surface modifications. Analysis of Subset 1 material identified a highly fragmented assemblage with a significant bias towards *Stegodon*. A large portion of these bones were likely fractured by trampling prior to entering the fluvial channel and were transported away from the death-site, undergoing surface modification causing rounding. Subset 2 material was less likely to have been transported far based on its limited susceptibility to fluvial transport. There was no significant difference in weathering for the long limb bones and fragments, with the highest portion exhibiting Stage 2 weathering, indicating that prior to final burial, all material was exposed to prolonged periods of surface exposure. Approximately 10% of all material have characteristics of fracturing on fresh bone, contributing to the taphonomic context for this bonebed; however insufficient evidence was found for anthropogenic modification.

**Keywords:** taphonomy; *Stegodon*; Middle Pleistocene; hominins; Flores; fluvial; bonebed; Mata Menge; southeast Asia



**Citation:** Powley, M.J.; Sutisna, I.; Mikac, K.M.; Wibowo, U.P.; van den Bergh, G.D. The *Stegodon* Bonebed of the Middle Pleistocene Archaeological Site Mata Menge (Flores, Indonesia): Taphonomic Agents in Site Formation. *Quaternary* **2021**, *4*, 31. <https://doi.org/10.3390/quat4040031>

Academic Editors: Juan Rofes, Janine Ochoa and Emmanuelle Stoetzel

Received: 1 July 2021  
Accepted: 10 September 2021  
Published: 29 September 2021

**Publisher's Note:** MDPI stays neutral with regard to jurisdictional claims in published maps and institutional affiliations.



**Copyright:** © 2021 by the authors. Licensee MDPI, Basel, Switzerland. This article is an open access article distributed under the terms and conditions of the Creative Commons Attribution (CC BY) license (<https://creativecommons.org/licenses/by/4.0/>).

## 1. Introduction

Extensive excavations from the early Middle Pleistocene archaeological site of Mata Menge, located near the northwestern margin of the So'a Basin, a ~400 km<sup>2</sup> depression on the island of Flores, Indonesia (Figure 1), have yielded in situ lithic artefacts and fossil vertebrate remains. The island is situated between the zoogeographical boundaries recognised as Wallace's Line in the west and Lydecker's Line in the east, in the region known as Wallacea. Flores has remained isolated from other landmasses even during periods of maximum low sea levels. The resultant low diversity fossil fauna was first examined in the 1950s when large fossilised bones, exposed by erosion, were excavated by Father Theodore Verhoeven, a priest affiliated with a nearby seminary, and identified

as *Stegodon trigonocephalus florensis* [1,2]. The continued work for more than two decades uncovered a large assemblage of *Stegodon* remains, other vertebrate fauna, and stone artefacts at various localities, including Mata Menge (Figure 1), the site that is the focus of our paper [3–5]. Analysis of the abundant fossil material allowed the attribution of the Flores *Stegodon* to a distinct species, *Stegodon florensis*, which is smaller than *Stegodon trigonocephalus* from Java [6]. During the 1980s and 1990s, an Indonesian-Dutch team carried out investigations into the claims of Verhoeven that hominins had colonised Flores during the Pleistocene [5,7]. Since 1997, systematic excavations at Mata Menge and other sites have occurred, leading to chronometric age determinations and further validation of Verhoeven’s findings, including details on the endemic insular fauna associated with stone artefacts embedded in stratigraphy representing over a million years [3,8–14]. Clear evidence for hominin occupation on Flores has been identified at various sites, including at two stratigraphic levels at Mata Menge, separated by 10 m of stratigraphy. A Zircon Fission-track age of  $0.80 \pm 0.07$  Ma for the Lower Fossil-bearing Interval (LFI) has been reported [13]. A more recent palaeomagnetic study [15] revealed that the LFI has a normal polarity and corresponds with the base of the Brunhes Normal Epoch. The LFI is therefore thought to be slightly younger than the Matuyama-Brunhes boundary at 0.773 Ma, which is within the error range of the ZFT age. The Upper Fossil-bearing Interval (UFI) is bracketed by ages of 0.78 and 0.65 Ma [10,13,15]. At the nearby site Wolo Sege, stone artefacts occur directly below a widespread pumice tuff layer, dated at 1.0 Ma [9] and, combined with the evidence from Liang Bua [16], indicates hominin occupation on the island for at least one million years.

However, only limited detailed taphonomic analysis of all fossils located in the LFI and UFI has occurred. A taphonomic study on *Stegodon* fossils from the LFI suggested that the *Stegodon* bones had been affected by fluvial transport [4]. Two additional studies focusing on avian remains from the LFI found several bone surface modifications, including parallel grooves, spindle-like striations, and rows of pits, but no unambiguous evidence for modifications made by hominins [17,18]. Taphonomic observations and analysis of the fossilised material, as well as the study of sedimentological features, can improve the interpretation of the context and significance of the hominin activities.

As mentioned, to date, no proof has been found that the Mata Menge hominins were involved in scavenging or hunting activities of fauna despite the co-occurrence of stone artefacts [10,17]. In 2014 the UFI yielded a fragment of mandible and six isolated teeth from at least three small-bodied hominins [14], which consolidated previous evidence for the presence of hominins at Mata Menge. These fossils established Mata Menge as the site containing the oldest hominin remains on Flores that likely represent the ancestral population of *Homo florensiensis* [14], the small-bodied hominin from the Late Pleistocene of Liang Bua cave, which is located 70 km WNW of Mata Menge. Here we present a preliminary taphonomic analysis of the Mata Menge vertebrate fossils to clarify some of the taphonomic processes that have contributed to the formation of the bonebed and investigate potential evidence of hominin modification of the *Stegodon* bones.

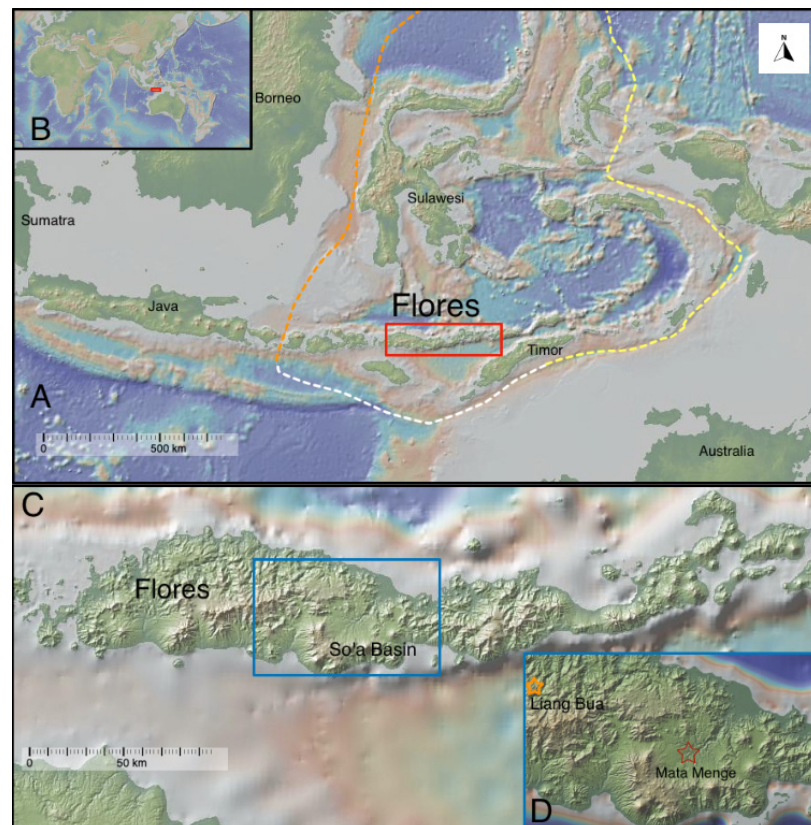


**Figure 1.** (A) Location of Flores (red rectangle) within the Indonesian archipelago. The orange line represents Wallace's Line; the yellow line represents Lydekker's Line; the white line connecting them represents the southern boundary of Wallacea [19]. (B) Location of the Indonesian archipelago. (C) Location of the So'a Basin (blue rectangle) on Flores, (D) Location of Mata Menge (red star) and Liang Bua (orange star) in the So'a Basin. (Map made with GeoMapApp ([www.geomapp.org](http://www.geomapp.org))/CC BY (accessed on 15 February 2021)).

### 1.1. Geological Context

The stratigraphic sequence that fills the So'a Basin consists of a basement substrate known as the Ola Kile Formation (OKF) deposited by volcanic events with a total thickness of at least 100 m [4,9]. A fission track age of  $1.86 \pm 0.12$  Ma for a tuff located at the top of OKF provides maximum age for the basin-fill sequence [13]. The Ola Bula Formation (OBF) sits unconformably on the slightly dipping OKF, with a maximum thickness of 120 m of volcanoclastic, fluvial, and lacustrine deposits [10] (Figure 2).

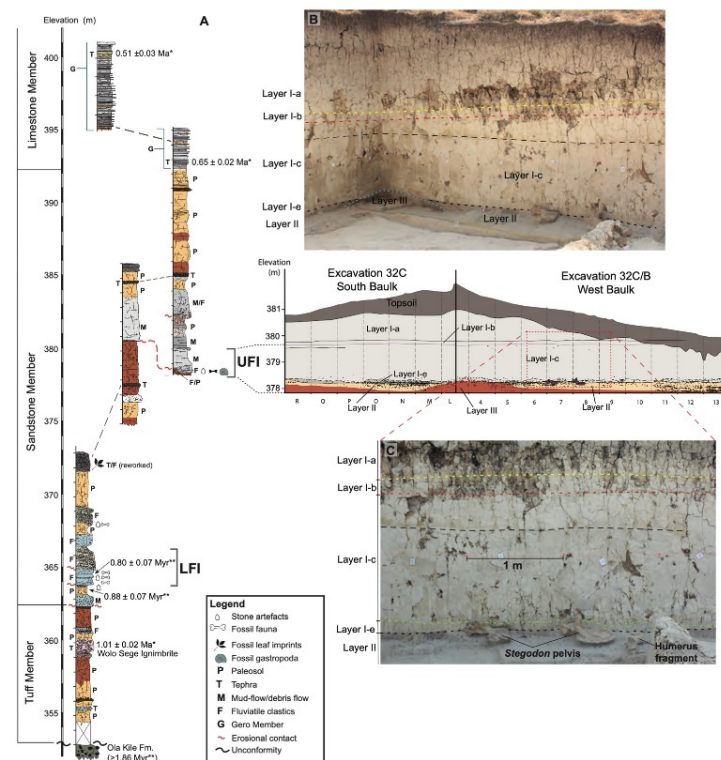


**Figure 2.** (A) Stratigraphy and chronology of the main fossil-bearing intervals at Mata Menge (Upper Fossil-bearing Interval, UFI, and Lower Fossil-bearing Interval LFI) as well as several basin-wide key marker tephra beds. (B) Photos and line drawings of the excavation baulks of Sector 32C (see also Materials and Methods for a plan view) in the UFI. The upper photo shows the view towards the SW corner of Sector 32C in 2015 when the up to ~30 cm thick sandstone lens that constitutes the main bonebed in the UFI (Layer II) was partly exposed. Layer II is overlaid by a sequence of massive, clay-rich mudflows (Layers I-a–e). Layer II has an erosional base and is deposited on top of a reddish paleosol (Layer III) with an irregular top surface, an elevated part of which is exposed in the corner. The line drawing in the middle shows the profiles of the south and west baulks in 2016 when Layer II was fully exposed in Sector 32C. (C) The bottom photo shows a detail of the west baulk. Two *Stegodon* pelvis bones and a humerus diaphysis are partly embedded in the sandstone of Layer II and are covered by the base of a 10 cm thick mudflow, Layer I-e, which contains abundant intraclasts eroded from the underlying strata and small fossils. Layer 1-d is not developed in Sector 32C, and Layer 1-e is here directly overlain by the massive mudflow unit Layer 1-c.

The OBF basal Tuff Member is characterised by an alternation of felsic pumice mass-flow layers and air-fall tephtras, reworked tuffaceous silts, sandstones, and conglomerate lenses [13,20]. This part of the sequence was deposited by infrequent volcanic events and braided river systems, with minor lacustrine/palustrine conditions. However, deposition was interrupted by long periods of non-deposition, as evidenced by the development of pronounced palaeosols [4,10]. A widespread marker bed located within this basal Tuff Member named the Wolo Sege Ignimbrite has been  $^{40}\text{Ar}/^{39}\text{Ar}$  dated at 1.01 ( $\pm 0.02$ ) Ma [9,10]. Only a single bonebed at the site Tangi Talo has been discovered within the Tuff Member, whereas stone artefacts have been shown to occur in fluvial conglomerates and associated overbank deposits just below the Wolo Sege Ignimbrite, providing a minimum age of ~1 Ma for the presence of hominins on the island [9]. The fauna from the bonebed at the locality Tangi Talo is characterised by few vertebrate taxa, with a giant tortoise, a 1 m tall pygmy proboscidean (*Stegodon sondaari*), and Komodo dragons (*Varanus komodoensis*), indicative of insular conditions [6,9,21].

The middle OBF Sandstone Member is characterised by sheet flow deposits, tuffaceous fluvial sandstones and siltstones, mudflow deposits, conglomerates, and a few mafic

tuff layers [10,11,22]. This unit was deposited by a fluvial system and includes channel deposits, overbank deposits, and mudflows, and again frequently overprinted palaeosols. Compared with the basal Tuff Member, a decrease in volcanic events was noted during the deposition of this member [4]. More frequent fossil beds are found in the sandstone member, commonly associated with stone artefacts. Zircon fission-track samples collected in the Sandstone Member date the deposits between  $0.88 \pm 0.04$  Ma and  $0.70 \pm 0.07$  Ma, aligning closely with  $^{40}\text{Ar}/^{39}\text{Ar}$  dated samples at  $0.81 \pm 0.04$  [10,12,13]. Both fossil-bearing intervals near Mata Menge occur in this stratigraphic unit.

The OBF is capped by the Limestone Member featuring thin-bedded micritic freshwater limestones, thin-bedded silty clay layers, and numerous predominantly mafic air-fall tephra layers [10,20]. Deposition in this member was dominated by lacustrine conditions and volcanic ash influxes [4]. A tephra sample from the top of this member gave an  $^{40}\text{Ar}/^{39}\text{Ar}$  age of  $0.51 \pm 0.03$  Ma [10] and another sample from the base of this member, taken at 14 m above the UFI, provided an  $^{40}\text{Ar}/^{39}\text{Ar}$  age of  $0.65 \pm 0.02$  Ma [10], in accordance with two zircon fission-track samples from within the member that returned ages of  $0.68 \pm 0.07$  Ma and  $0.65 \pm 0.07$  Ma. Along the basin margins, the top of the OBF is overlaid by volcanoclastics from volcanoes surrounding the basin, some of which are still active [20].

### 1.2. Stratigraphic Context for Mata Menge

The Lower Fossil-bearing Interval (LFI), bracketed by a maximum age of 0.78 Ma based on palaeomagnetic evidence and a minimum age of 0.81 Ma [15,23], contains impoverished vertebrate fauna as well as in situ stone artefacts. The up to 2.2 m thick LFI represents a fining-upward sequence consisting of an amalgamated complex of sheets and lenses of sandstone alternating with tuffaceous siltstones and clay-rich mudflows. While no fossilised hominin remains, or evidence for hominin butchery practice have been identified from the LFI, simple stone technology excavated from this interval provided proxy evidence for the presence of hominins [4]. A taphonomic analysis on the *Stegodon* bone assemblage from the lower interval indicated that fluvial transport had removed smaller and more easily transportable bones from the assemblage, especially from the high-energy erosional basal sandy layer [4]. Additional excavations in the lower interval did not yield any hominin remains, and during 2013 fieldwork, excavations were expanded to a sandstone layer 10 m higher in the stratigraphic sequence, to what has been referred to as the c. 100,000 years younger Upper Fossil-bearing Interval (UFI) [10]. The fossil-bearing layer here comprises a less than 30 cm thick sandstone lens.

The sedimentology of the Upper Fossil-bearing Interval (UFI) has been described to some extent in a previous paper [10]. The fossils are concentrated in a sandstone layer (Layer II) with an erosive base, which fills in an irregular topography of a well-consolidated palaeosol (Layer III; Figure 2). Layer II has a maximum thickness of ~35 cm and wedges out towards the western margin of the site. Layer II consists of medium-coarse, poorly sorted sand with scattered rounded pebbles at the base. The average maximum diameter of the 15 largest pebbles is 91 mm (the largest pebble had a diameter of 115 mm). Using a Hjullström diagram, this would indicate a current transport velocity of over 100 cm/s to allow transport of such pebbles to the site. Layer II is fining upwards to medium to fine-grained sand at the top, suggesting decreasing flow velocity when the layer was deposited. Internal sedimentary structures are generally absent apart from vaguely preserved parallel laminations at the basal part of the layer. Layer II is covered by a 6.5 m thick series of massive clay-rich mudflow deposits (Layers I-a to I-f), which also contain few small fossil bone fragments and rounded mud intraclasts at the base. This sequence has been interpreted as the deposit of a small stream on a distal volcanic apron, cutting into consolidated palaeosol deposits, and at some stage rapidly covered by a series of mudflows, which most likely originated from a caldera structure with a lake directly north of Mata Menge [10]. It is notable that articulated fossils are very rare and that many *Stegodon* fossils show signs of rounding by fluvial transport. Some of the larger *Stegodon* fossils are half embedded in the fluvial sandstone and are covered by the mudflow (see Figure 2, lower

photo). For the assemblage studied here, only fossil specimens from the sandstone Layer II were included in the analysis.

### 1.3. Location and Fauna

The isolation of Flores within the zoogeographical borders of Wallacea during maximum glacial events throughout the Pleistocene restricted access to the island to animals that could either fly, raft, or swim there (Figure 1) [7]. Endemic vertebrate fauna excavated from both levels at Mata Menge is restricted to *Stegodon florensis*, crocodile, *Varanus komodoensis*, a single giant rat species *Hooijeromys nusatenggara*, various types of birds, and frogs [4,10,17,24]. *S. florensis* is larger than *S. sondaari* from the underlying Tuff Member and represents a new immigrant to Flores, replacing *S. sondaari*. The Mata Menge *S. florensis* has been classified as a separate chrono-subspecies that was ancestral to *Stegodon florensis insularis* from the Late Pleistocene of Liang Bua [25].

From the thousands of fossils already excavated on Flores, no evidence for the presence of large mammalian predators has been found to date. Between 2010 and 2019, over 33,000 fossils were unearthed from excavation sites across the So'a Basin [26]. Of the fossil assemblage excavated from the UFI at Mata Menge until 2015, the largest portion comprised unidentified bone fragments (~44%), while the remainder of the fossils could be identified to the class taxonomic level. These relative proportions changed little after additionally incorporating the UFI fossils excavated during the period 2016–2019, totalling 15,535 specimens, which can be attributed as follows: unidentifiable fragments (42.9%); *Stegodon* (33.9%); Murine rodents (19.0%); Crocrodilia (2.0%); Varanidae (0.68%); other Reptilia (0.7%); Aves (0.56%); Anura (0.28%); and Hominin 0.06% [26].

The bonebed at Mata Menge is important for interpreting formation processes of bonebeds that have no modifications made by mammalian carnivores. There are many continental examples of proboscidean bonebeds that have been modified by mammalian carnivores to various degrees, largely through disarticulation and dispersal of carcasses and bone surface modifications such as teeth punctures or gnawing on bone ends [27–30]. At Mata Menge, reptiles were the primary faunal predators. Reptilian predators can remove bones completely from the assemblage through digestion [31,32], or residual bones may retain bone surface modifications. Some researchers have suggested that the V-shaped linear grooves made by crocodile teeth cannot always be distinguished from those made by stone tools [33] unless advanced statistical tests are applied [34].

The question of whether hominins were involved with the accumulation of faunal remains here or what other agents led to their preservation remains unresolved at this time. Large numbers of *Stegodon* fossils, some with reported cutmarks, and evidence of anthropogenic bone accumulation of insular fauna attributed to *H. floresiensis* were identified at Liang Bua, revealing substantiation of hominin modification of *Stegodon* remains during the Late Pleistocene [35]. Whether hominins used stone artefacts with similar technology identified in both locations, which are separated in time by ~600,000 years [8,10], to hunt, scavenge/butcher, and consume *Stegodon* is one of the key motivators of this research. *Stegodon*, the largest fauna element on Flores during the Middle Pleistocene, could have provided substantial amounts of meat to hominins, which may have contributed to the decision to hunt this species. However, evidence for meat consumption by the Early to Middle Pleistocene hominins has so far not been uncovered at Mata Menge. In order to begin to interpret the material from the UFI at Mata Menge, analysis for this research was focused on identifying the presence of fractures on fresh bones, bone surface modifications and subsequently identifying the extent of surface exposure and possible fluvial transportation of the bones, processes that may have obliterated bone surface modifications.

### 1.4. Taphonomic Processes

Biological processes, including modifications made by hominins for food procurement and butchery [8,36–39], the use of bones as tools [40,41], and anthropogenic bone accumula-

tion [25,42], have characteristics recognisable through the analysis of bone fracturing, bone surface modification, and location of bones in a bonebed. Similarly, faunal modifications are identified by characteristics on the bones that are associated with predation and feeding. Vertebrate tooth marks [31,34,43,44], disarticulation patterns such as those from large reptiles [34,43], and even the absence of bone material from the site when bones are completely removed through digestive corrosion [34], can provide additional context and contribute to the identification of vertebrate modification of bones. Additionally, proboscidean assemblages may include taphonomic modifications through the process of trampling. Based on observations of modern elephants, *Stegodon* are likely to have repositioned bones of deceased animals with their feet and trunks. The fracturing of complete elements and increased fragmentation through continued trampling on the bones is highly likely to have occurred. Fully or partially submerging of bones below the ground surface due to trampling may have caused variable exposure to weathering for both the whole carcass as well as the individual skeletal elements. This is an additional taphonomic processing possibility [45].

Non-biological taphonomic processes likewise have characteristic features that are observable on fossilised material from bonebeds. Significantly for the Upper Interval at Mata Menge, evidence to support deposition by a small sinuous stream tributary identified by the occurrence of in situ water-worn volcanic pebbles, as well as locally faint parallel laminations in the lower part of Layer II, was previously reported [10]. Bones deposited in fluvial systems experience characteristic modifications, including bone rounding and abrasion of the bone surface, causing loss of anatomical features and other taphonomic surface modifications [46–48]. Bones entering a fluvial system are also susceptible to transport potential based on the type and size of element or body part [47–51], the intact nature of the bone [52], and the fluvial velocity [53]. Analysis of the extent of weathering on the bone while on the surface was performed to evaluate the consistency of weathering from across the site as an indicator of the amount of exposure the fossils experienced prior to either partial or final burial [49,54–56]. All the potential pre-burial taphonomic processes at Mata Menge are thought to have ceased abruptly after 6.5 m thick mudflows sealed off the sandstone layer and the bones that were present on the surface at the time.

## 2. Materials and Methods

### 2.1. Materials

Material from this preliminary study was excavated between 2013 and 2018 by a team of Indonesian and Australian researchers and is stored at the Geological Museum Bandung. Two representative subsets were selected for detailed analysis. Subset 1 included all vertebrate fossils excavated from two adjacent one-metre quadrants on the eastern margin of a 3-metre-wide stream gully infill (Layer II, quadrants O5-O6; see Figure 3). At this sampling spot, Layer II laps on against an elevated crest of the erosional subsurface palaeosol (Layer III), and three of the five hominin fossils that were not recovered during wet sieving, were retrieved from this stream gully infill, including a premolar from quadrant O6. Therefore, this area was chosen for the Subset 1 sample because the taphonomic analysis might provide clues as to why the hominin fossils were concentrated in this gully. The sample also contains fossils of all the most abundant taxa at Mata Menge and is representative of the fauna present in Layer II. Subset 2 included all *Stegodon* long limb bones and limb bone fragments excavated from Layer II of the Upper Interval at Mata Menge ( $n = 17$ ). Although axial skeletal elements, ribs, and bones of the manus and pes are present in the assemblage, only the long limb bones (femur, tibia, fibula, humerus, radius, ulna) were chosen because certain types of butchery marks and indicators of hominin food procurement can be preserved on these representative proboscidean skeletal elements [41,57–61]. Accessing the medullar cavity for the consumption of highly nutritious marrow has been claimed at other proboscidean kill sites, and such activities could have left diagnostic fresh bone impact marks and fracture patterns on the long limb bones [60–62].

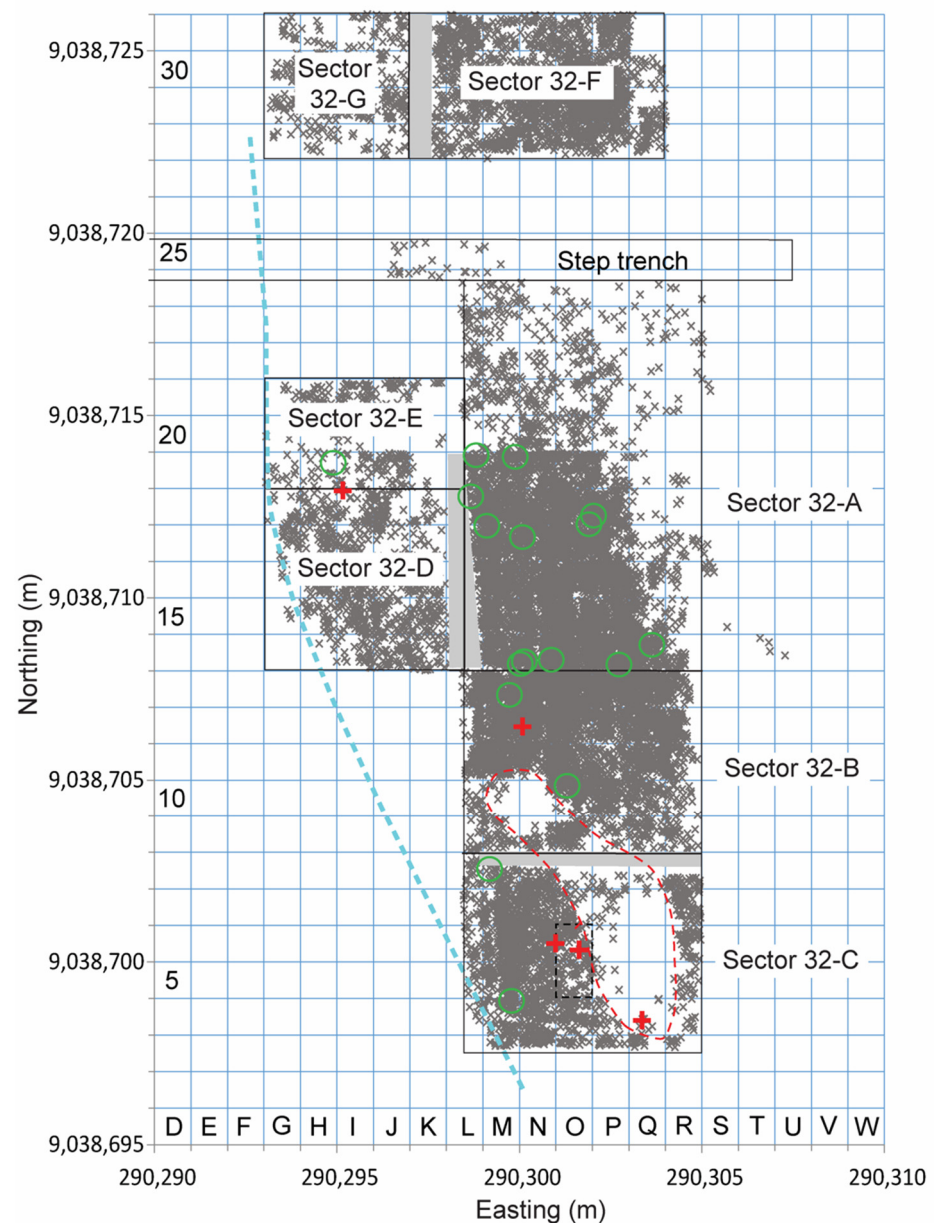


**Figure 3.** Plan view of the sectors of Excavation 32 in the Upper Fossil-bearing Interval at Mata Menge. Green circles indicate locations of Subset 2 long limb bones used in this study; red crosses indicate hominin fossil locations; grey crosses represent locations of all fossil specimens. The blue dotted line indicates the western termination of Layer II, where it pinches out against the elevated substratum of Layer III. This has been interpreted as the lateral bank of the fluvial stream channel. The black dotted rectangle indicates the location of the Subset 1 assemblage. Blue squares represent 1 m<sup>2</sup>. Note that the northern half of Sector 32A and Sector 32B have been excavated to the base of Layer II, hence showing less dense spacing between finds. The area indicated with a red dashed line represents an elevated part of the eroded substratum of Layer III, where Layer II is thinner or absent, thus showing fewer fossils. Grey areas were not excavated.

## 2.2. Taphonomic Analysis

Identification of fossilised material was undertaken at the Geological Museum Bandung using *E. maximus* and *E. hysudrindicus* material for comparison. Fragments of bone with a cortical thickness greater than 4 mm were examined for characteristic crocodilian growth rings [63] and, if absent, the fragment was attributed to *Stegodon*. Enamel and tusk fragments were identified by their colour, texture, and shape, distinguishing them from

fragmented bone. *Stegodon* enamel, usually thicker than 1 mm, has a translucent, double-layered, and wrinkled appearance [6] and is usually easy to distinguish from tooth enamel of other vertebrates, even tiny fragments. *Stegodon* tusk consists entirely of dentine, which is not covered with enamel but has a regular intersecting arcuate pattern in cross-section, referred to as Schreger Bands [64], which enabled macroscopic identification.

All fossils were examined macroscopically and, where required, with a handheld lens at 10× magnification. A caliper was used to take size measurements of all materials. The fossils of Subset 1 were measured along the longest length of the fossil to determine the Fragmentation Size Class [59]. The extent of fragmentation within a bonebed can be measured by comparing the number of Whole Bones and Part Bones with the remaining number of fragmented bones in the bonebed. Whole Bones are complete and unbroken (including complete teeth), whereas Part Bones represent fossils that constitute more than half of a recognisable bone element [58]. For example, a proximal portion of a long limb bone that was at least half of the original element was classed as a Part Bone. All material was assigned to one of ten size classes, based on the completeness of the bone element or its length (>10 mm, 10–20 mm, 20–30 mm, 30–40 mm, 40–50 mm, 50–60 mm, 60–70 mm, 70–80 mm, Part Bone, and Whole Bone).

Bone fractures were compared with descriptions defined by Outram [65] and were allocated a Fracture Freshness Index score of FFI 0–6. Although this analysis technique was not developed using proboscidean material, successful application has been observed on several large mammal species, including a preliminary review of mammoth material [66–71]. Criteria to define the FFI are Fracture Angle, Fracture Outline, and Fracture Texture, and were based on visual examination. For each of these three criteria, a score of 0, 1, or 2 was allocated for each specimen. A score of 0 was given if the fossil had only features indicative for fresh bone fracturing, a score of 1 if mixed fresh and unfresh fracture characteristics were present on a single specimen, and a score of 2 if only unfresh fractures could be determined. Consequently, a combined minimum FFI score of 0 would indicate all fractures occurred while the bone was fresh; alternatively, a maximum score of 6 indicates all fractures occurred while the bone was dry or fossilised.

Any fractures or surface modification attributed to sullegic or trephic processes were not included in FFI (or other palaeontological) analysis but were recorded separately. These modifications were clearly identifiable due to their characteristic fracturing patterns on fossilised material, usually following existing drying cracks and as a result of vibrations resulting from hammers and chisels used to break through the cemented sandstone in which the fossils were embedded. This process then exposed underlying material that was typically a different colour when compared with the outside of the fossil or old fractures.

All bones from both subsets were allocated a Stage of Weathering based on their physical characteristics described by Behrensmeyer [54], Stage 0–5:

Stage 0—No signs of cracking or flaking, bone may have tissue attached;

Stage 1—Cracking usually seen parallel to fibre structure, also mosaic cracking;

Stage 2—Outer bone show flaking, long thin to extensive flaking;

Stage 3—External bone patchy to mostly removed;

Stage 4—Coarsely fibrous rough bone surface, cracks well opened; or

Stage 5—Bone is fragile and easily broken, loss of original bone shape possible.

Other surface modifications, including biting and gnawing marks, dynamic impact marks, striation marks, corrosion, and abrasive rounding, were noted as absent or present. Residual sediment attached to Subset 1 fossils was macroscopically assessed for and allocated into very coarse to coarse, medium, or fine-grained to very-fine-grained sand categories according to the Wentworth Scale.

### 3. Results

#### 3.1. Subset 1-Assemblage

The Subset 1 material attributed to *Stegodon* was 78 out of 91 (86%) fossils. The second-highest portion was Murinae (9%), followed by *Crocodylus* (4%) and hominin (1%).

Approximately 54% of the highly fragmented *Stegodon* material was represented by unidentifiable bone fragments, where the provenance of the skeletal element was impossible to determine. The next highest portion of identifiable *Stegodon* fragments were very small fragments of tusk (21%) and tooth enamel (11%), but no complete or partially complete *Stegodon* tusks or teeth were identified from the subset (although scattered complete dental elements are present in Layer II). The remaining *Stegodon* fragments were small fragments of costa (5%), cranium (5%, consisting of cranial fragments characterised by thin-walled pneumatic bone tissue), and a single complete hyoid bone. Of the Murinae fossil material, 74% were either tooth or long bone fragments.

### 3.1.1. Fragmentation Analysis

Of the 91 fossils in Subset 1, extensive fragmentation was identified (94%). The 6% that was not fragmented included Part Bone classified teeth from *Crocodilus* and Murinae, as well as a single complete *Stegodon* hyoid bone. The majority of fragments were in the 10–20 mm class, followed by the 20–30 mm class and the <10 mm class, respectively. Combined, these classes represented 86% of all the fossils from Subset 1 and, additionally, 75% of fragments under 30 mm in length were attributed to the largest animal in the bonebed, *Stegodon*, based on the thickness of the cortical bone (Figure 4).

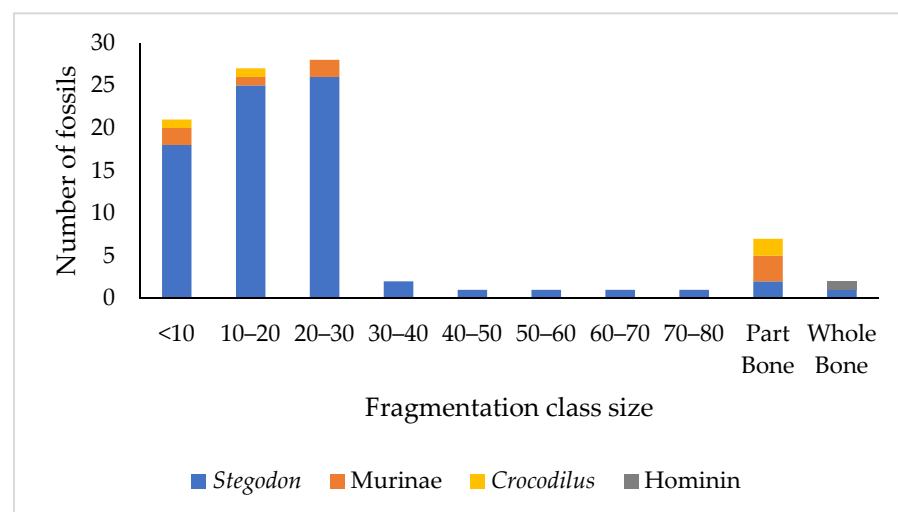


**Figure 4.** Results for analysis of the Fragmentation Classes of bone complete elements and bone fragments for Subset 1 ( $n = 91$  NISP). Classes up to 80 mm are bone fragments. Part bone is more than half the original bone, and whole bone is entirely unbroken bone element. Portions of the column in various colours are representative of each identified species.

### 3.1.2. Weathering

None of the Subset 1 material was found to be in fresh or unweathered condition. The highest portion of fossils was Stage 2 weathering (56%), followed by Stage 1 (21%) and Stage 3 (16%); the remaining (3%) were each Stage 4 and Stage 5 (Figure 5). A significant difference was found ( $\chi^2 (4,91) = 13.135, p = 0.01, n = 91$ ) when attributing fragmented material to a skeletal element for less weathered fragments, indicating that an increase in weathering on fossils reduces the likelihood of it being identified. No fragment from Subset 1 was identified to a skeletal element in Stage 4 or Stage 5 weathering.

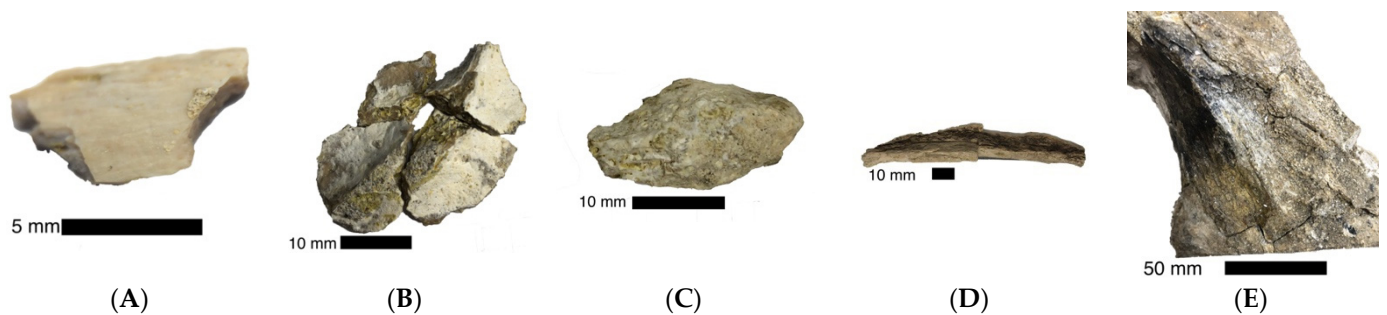


**Figure 5.** Stages of Weathering from Subset 1 assemblage. (A) Fossil ID MM14-F392, Stage 1 weathering, the outer bone surface shows some small mosaic cracks (fracture edges a result of excavation damage). (B) Fossil ID MM14-F1389, Stage 2 weathering, moderate outer bone flaking. (C) Fossil ID MM16-4515, Stage 3 weathering, cortical bone patchy and mostly removed (D) Fossil ID MM14-F106, Stage 4 weathering, coarse fibrous bone exposed due to external cracks. (E) Fossil ID MM16-F4505, Stage 5 weathering, loss of original bone shape, and easily broken.

### 3.1.3. Bone Surface Modifications

No evidence of any biting or gnawing marks on the material was observed. No dynamic impact marks were observed on bone material that was likely to have been anthropogenic. The three incidents of crush style fractures had characteristics consistent with dry bone fracturing, and therefore are likely to have been caused by trampling. There were three *Stegodon* bone fragments with one or more linear surface marks. One costa fragment in weathering Stage 1 had multiple curved surface scraping style marks as well as two perpendicular parallel marks that contained in situ matrix within them (Figure 6). No evidence of any digestive corrosion was seen on any material. Moderate to heavy black staining penetrating the fossil bone surface up to 5 mm was seen on 55% of all material. These findings suggest that the bones have been exposed to dissolved manganese minerals in the water in which they were (intermittently) submerged [17]. There were incidents of dissolution circular pitting seen on the hominin premolar and some fossil surfaces (Figure 7). Some fragments presented with completely rounded edges, likely the result of abrasion during fluvial transportation, but further microscopic analysis would be required to confirm this (Figure 8). Macroscopic grain size assessment of the residual matrix on the Subset 1 fossils showed that 84% of the fossils had a matrix consisting of fine-grained sand, indicating that these fossils originated from the top of Layer II. A total of 14% was poorly sorted coarse-grained sand, and the remaining 2% was medium-grained sand.

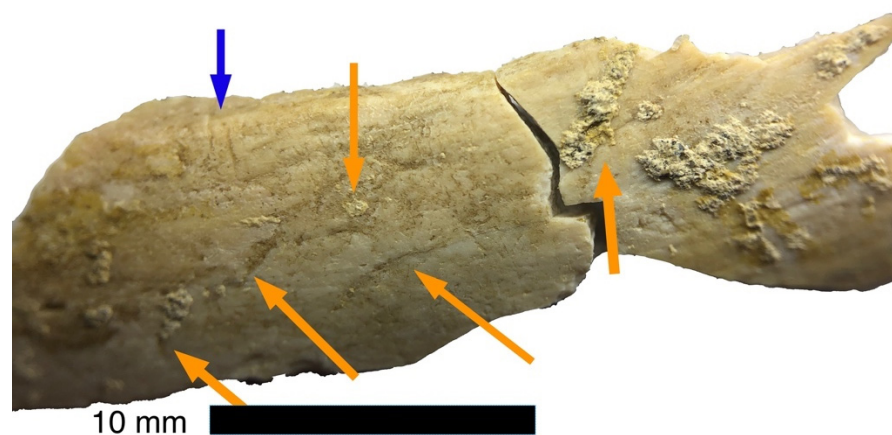


**Figure 6.** Fossil ID MM14-394 *Stegodon* costa bone broken in two by excavation fracture with perpendicular parallel narrow striations (blue arrow), curved scrape type marks (orange arrows), some with in situ matrix are present.

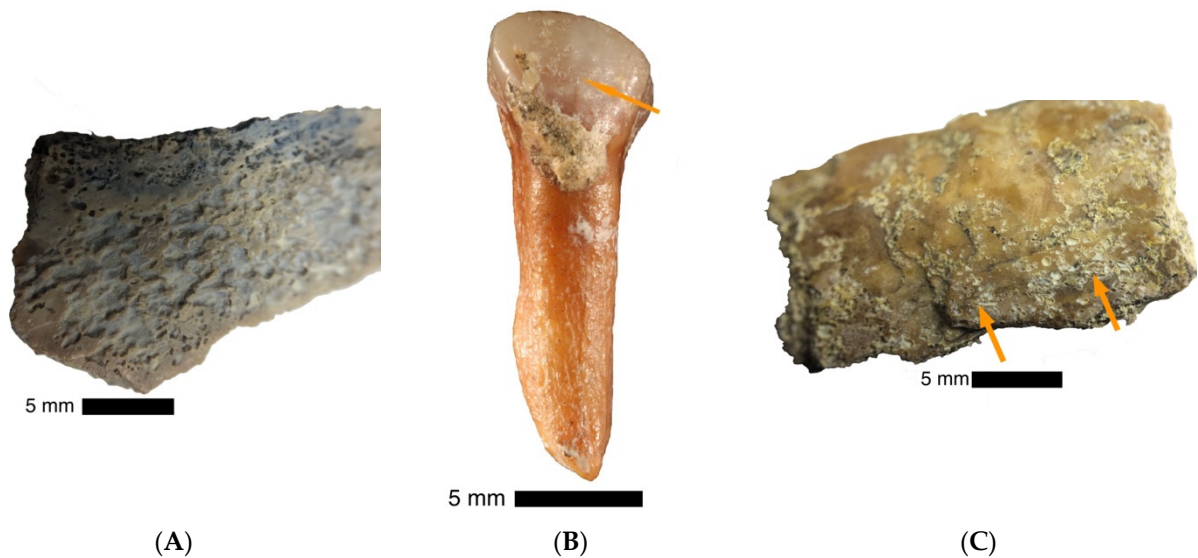


**Figure 7.** Examples of dissolution circular pitting from Subset 1 assemblage. (A) Fossil ID MM14-F149 small fossilised *Stegodon* tusk fragment showing irregular dissolution pattern. (B) Fossil ID SOA-MM5, Hominin premolar with dissolution circular pitting (orange arrow) (Photo source: Kaifu 2016). (C) Fossil ID MM14-F1316, *Stegodon* bone fragment with multiple circular dissolution pits (orange arrows).

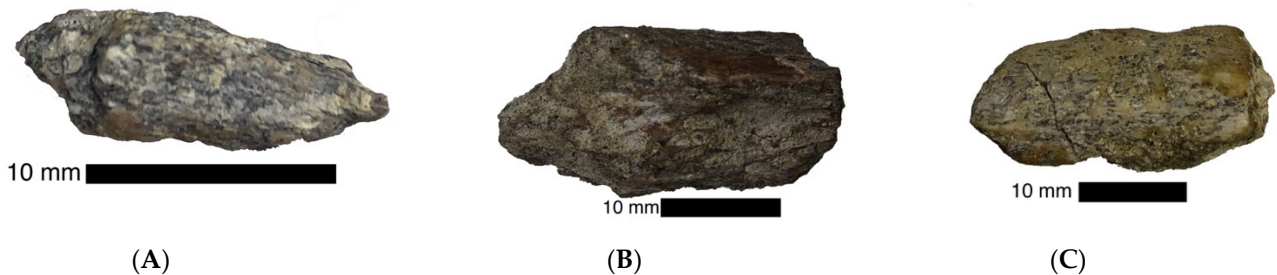


**Figure 8.** Examples of rounded fragments from Subset 1 assemblage likely as a result of abrasion in fluvial transportation. (A) Fossil ID MM14-F348, *Stegodon* bone fragment. (B) Fossil ID MM14-F487, *Stegodon* bone fragment, (C) Fossil ID MM14-F1413, *Stegodon* bone fragment.

### 3.2. Subset 2-Long Limb Bones

#### 3.2.1. Identification

From the Subset 2 *Stegodon* long limb bone analysis ( $n = 17$ ), 3 bones were complete elements, 10 were classified as Part Bones, consisting of at least half of the original element, and the remaining 4 were bone fragments. No elements from this subset were located in articulation. The most abundant element was the humerus, with three left and three right-side identified. There was a single complete humerus, and the remaining five were Part Bones. One left and one right complete femur was found; however, these were from different individuals as there was more than a 10 cm difference in length. Unpublished data from this site based on the identification of dental elements suggest an MNI of at least 35 individuals. The loss of postcranial material through transportation and fragmentation, following from the analysis of Subset 1 from this site, is therefore likely.

#### 3.2.2. Weathering

From the weathering analysis of Subset 2, no fossil was found completely unweathered (Stage 0 weathering). The highest proportion was Stage 2 (44%), followed by Stage 3 (28%), both Stage 1 and Stage 4 (11%), and the remaining was Stage 5 (6%). In order to refine the analysis of weathering on the bone only material, enamel and tusk fragments from the Subset 1 data set were removed, and statistical analysis was performed. There

was no statistical difference identified between Subset 1 and Subset 2 for weathering ( $\chi^2_{(4,74)} = 4.832, p = 0.30, n = 74$ ). There was no statistical difference identified for *Stegodon* only bone material between Subset 1 and Subset 2 for weathering ( $\chi^2_{(4,68)} = 5.053, p = 0.28, n = 68$ ). Two incidences of differential weathering were observed on the proximal and distal ends of two left ulnae from Subset 2. Both bones were Stage 2 proximally and Stage 4 or Stage 5 distally (Figure 9).

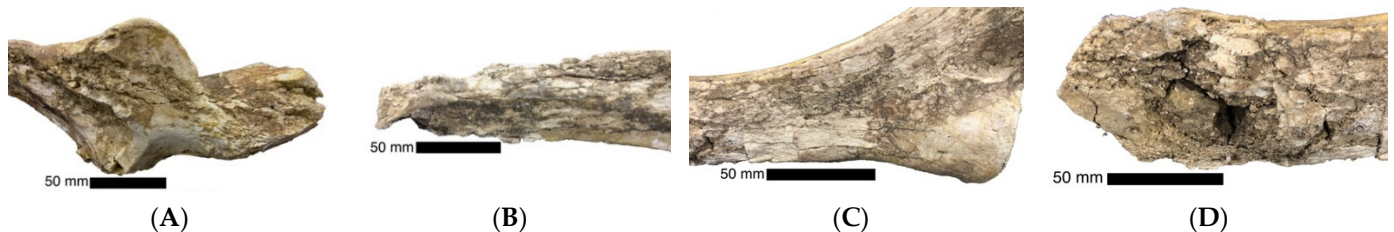


**Figure 9.** Differential weathering on two left ulna bones. Both proximal ends are less weathered when compared with the more pronounced weathering on the broken distal ends. Fossil ID MM13-F072 (A) Proximal. (B) Distal. Fossil ID MM13-F721 (C) Proximal. (D) Distal.

### 3.2.3. Fracturing

For both Subset 1 and Subset 2 fossils, the Fracture Freshness Index (FFI) score of 6 accounted for approximately 75% of the material. This indicates that all observed fractures occurred while the bone was either dry or fossilised, likely a result of non-anthropogenic modification. Of the remaining Subset 1 material, approximately 10% scored 3 or 4 on the FFI with both fresh and non-fresh fracture characteristics (Figure 10). No uniformity was detected in the fractures or their location on the Subset 1 fossils. For the FFI criterion Fracture Outline, a helically shaped fracture was observed on each of five humeri from Subset 2 (Figure 11). The humeri presented with the proximal portion of the bone missing and a helically shaped fracture differentially located along the shaft. In all cases, the anterior-medial aspect of the bone is the highest point of the fracture, and the lateral aspect is the lowest. Fractures were observed both proximal and distal to the deltoid tuberosity (Figure 11). However, the FFI characteristic evidence alone observed in either subset is not sufficient to confirm that the fractures occurred while the bone was fresh.

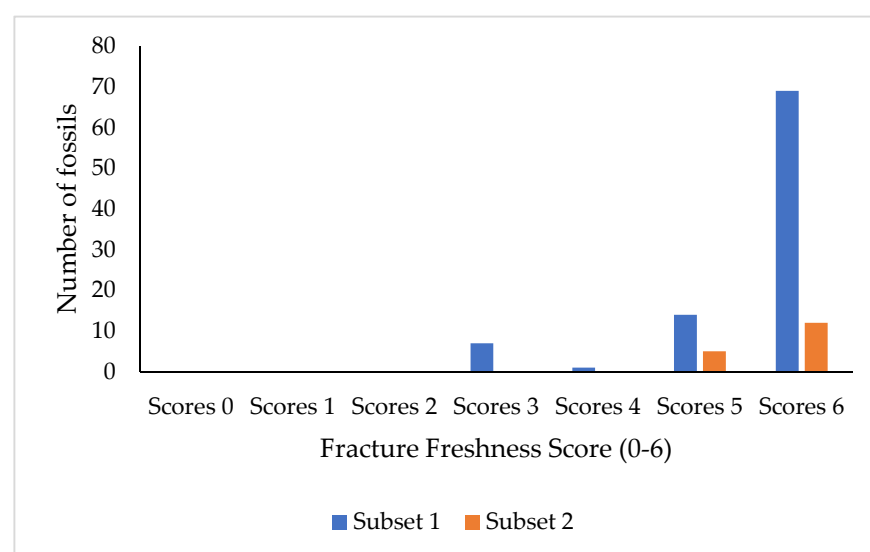


**Figure 10.** Numbers of fossils (NISP) in Subset 1 ( $n = 91$ ) and Subset 2 ( $n = 17$ , long limb bones) represented by Fracture Freshness Index (FFI) Scores 0–6. The highest portion of material Score 6 indicating all fractures characteristic for unfresh bone fracture. Approximately 10% of material scoring 3 or 4 on the FFI.

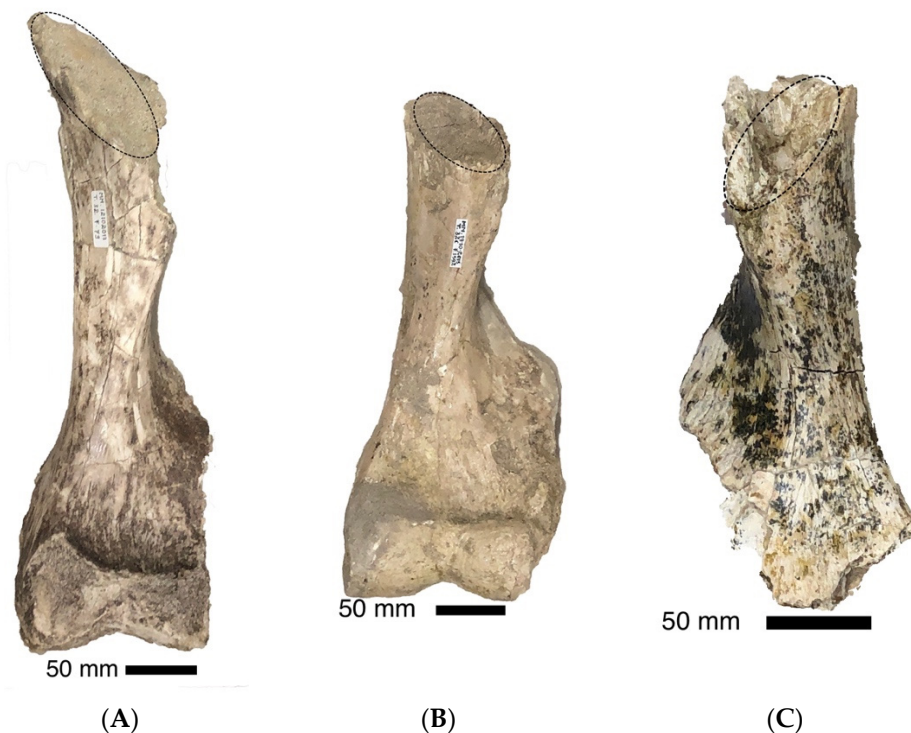


**Figure 11.** Examples of helical-shaped fractures on three humerus bones from Subset 2. The black outline represents the shape of the fracture. The highest point of fracture is medially, and the lowest point is lateral. Fracture presents both above and below deltoid tuberosity on different fossils. (A) Cranial view *Stegodon* Left humerus (MM13-179) (B) Cranial view *Stegodon* left humerus (MM15-1592). (C) Cranial view *Stegodon* right humerus (MM16-7610).

#### 4. Discussion

The analysis of the Subset 1 fossils from Mata Menge Upper Interval (UFI) has revealed a significant bias towards bone fragments of the largest taxon present. This is not surprising, as the comparatively robust nature of the *Stegodon* bones has contributed to their preferred preservation, representing 86% of the assemblage, despite the fact that many of these *Stegodon* fossils represent small broken fragments of unidentifiable elements. Smaller vertebrates are mostly absent from the fossil record here, likely because of their susceptibility to rapid degradation caused by weathering after Stage 2. This commonly observed feature was recognised by Behrensmeyer (1978), who noted that animals under 100 kg, and especially those under 15 kg, after undergoing surface weathering are usually under-represented in fossil assemblages. During Mid Pleistocene in the So'a Basin, many birds, reptiles, and murids would be classified in the small vertebrate class size, therefore likely undergoing fast decay and rapid full bone degradation during surface exposure.

More than half of the *Stegodon* fragments are fragments of cortical bone, similar to observations made at other proboscidean assemblages where large numbers of fragmented cortical bone were located [40,72]. No other species in the So'a Basin during the Mid Pleistocene were large enough to have cortical bone of this size [6,73]. The highly fragmented nature of the *Stegodon* material in the bonebed contributed to difficulties in attributing bone fragments to a skeletal element. There was no increase in the successful identification of fragments to a skeletal element as their size increased. No fragment could be identified when showing Stage 4 or Stage 5 weathering. Fragments without any recognisable skeletal bone characteristics have undergone considerable surface modifications such as those seen in weathered material; however, abrasion and rounding caused during fluvial transportation certainly contributed considerably to modifications observed on these fossils.

Fractures on fresh bones have a close association with the biological dispersal of a carcass [74,75]. Biological agents in the Soa Basin are represented by either a reptilian

carnivore, trampling, or other modification of dispersal by *Stegodon* or hominin. During Mid Pleistocene in the So'a Basin, the only faunal predators large enough to disarticulate and consume *Stegodon* included crocodiles and Komodo dragons [10]. However, these predators rarely fracture bones during feeding, preferring to either consume large disarticulated portions or complete smaller animals [31,33]. No evidence was found for any puncture style marks attributable to crocodile teeth. Ziphodont teeth of Komodo dragons are suitable for cutting flesh and not for puncturing bone. Based on the highly fragmented material in Subset 1 when compared to the selected complete element material from Subset 2, it is clear that the two subsets were exposed to different taphonomic processes by agents prior to entering the fluvial channel.

Five *Stegodon* humeri were observed with helical-shaped fractures located at various positions along the diaphysis of the bone. Observed fractures are located both proximally and distally to the deltoid tuberosity resulting in the differing presentations of these elements. While the helical nature of this fracture may not present sufficient evidence for the identification of a fracture occurring on fresh bone, the edges of these fractures were exposed to further taphonomic processes, including weathering and natural abrasion. These secondary processes have likely altered the fracture edge and reducing diagnostic interpretability. It is likely these fractures were the result of trampling, similarly observed on trampling fractures of modern elephants [45].

During recent actualistic experimentation and fieldwork observations in Africa with modern elephant bones (*Loxodonta africana*), the effects of trampling resulting in bone fractures were described [45]. Fractures due to trampling were observed in association with other bone surface marks, including scratches, grazes, and other marks distinguishable from cut marks. The fine-grained sand observed at the experiment location in Africa caused shallow, narrow, flat bottom marks that were multidirectional [45]. Acquisition of these marks was attributed to elephant trampling. While the characteristic trampling marks were not macroscopically observed on the fractured humeri from Mata Menge or on any of the long limb bones, conceivably, weathering and ablation may have obliterated scratches and grazes on the bone surface. The relatively well-preserved costa fragment from Subset 1 identified with multiple scrape marks were consistent with the description from experimental conditions and, therefore, likely the result of trampling; however, further microscopic analysis may provide additional context for this material.

Additionally, elephants frequently partially submerge bones in the sand surface, resulting in vertically reorientating the bones [45]. Some evidence supporting likely trampling-induced reorientation of bones was identified at Mata Menge with differential weathering observed on the proximal and distal ends of two *Stegodon* left ulna bones. Both ulnas had well-preserved Stage 2 weathering on the proximal end, while the distal ends of both bones were Stage 5 weathering. Intuitively, it is likely that the heavier and larger proximal end of the ulna bone could remain submerged after being pushed into the surface by force exerted by *Stegodon* feet, and therefore the proximal end remained protected from the exposure taphonomy of weathering.

Significant to the context for this bonebed is a further interpretation of the previously identified fluvial channel in which the fossils were preserved [10]. The sedimentology, identification of freshwater gastropods and water-worn volcanic pebbles led previous researchers to conclude that Layer II was deposited in a small stream [10]. The taphonomic analysis of the fossil assemblage is in accordance with this interpretation. The fragmented material in Subset 1 has undergone significant abrasion taphonomy and resulted in modified surface features caused by the significant removal of bone material in flowing water. The long limb bones underwent somewhat less abrasion in the fluvial channel, by comparison, resulting in some bone surface reduction, particularly on bone processus. Further interpretation of the two presentations of bone wear observed in this bonebed requires analysis of the mechanisms of the abrasion seen here. The mechanisms rely on the increasing hardness of the material and increasing velocity; however, whether the bone material was fresh or dry will influence the resultant abrasion [76]. Abrasion on

bone material that is more ductile, such as fresh bone, is a result of sharp, angular cutting from the sediment and results in ablation-induced surface bone removal. Abrasion on dry bone is the result of deformation around existing cracks and impact points on the less elastic bone; subsequently, intersecting cracks lead to fragmentation and detachment of material [76]. These described conditions are exacerbated by the length of exposure time in the fluvial environment. The Mata Menge UFI bonebed is made up of material with multiple taphonomic histories, including: condition of bone entering the fluvial channel; dry or fresh; and interval of exposure to the fluvial conditions and post mortem breakage, much of which should be attributed to trampling.

Susceptibility to transportation in a fluvial system was also observed here. Maximum cortical bone thickness is considered to positively influence the transportability of fragments in a fluvial environment [52]. The over-representation of *Stegodon* material, as opposed to fossils of smaller taxa, would therefore be in accordance with a fluvial setting. It is probable that smaller bone material, including cancellous bone fragments and material from smaller vertebrates, was transported away from this site, further contributing to the bias identified here. Dry bones have a high transportation potential [50] as they are inclined to float when compared to fresh bones, whose high moisture content makes them more likely to become submerged. The high density of comparable bone fragments in both size and type in the assemblage reveals the likelihood of fragmented bone entering the fluvial channel following significant fracturing processes. The fine-grained sand adhering to the majority of the fossil fragments indicates that they originate from the upper part of Layer II. Fine-grained sand related to slower fluvial transportation [46] is associated with more bone edge rounding on fresh bone when compared with either dry or fossilised material in experimental research [77]. Based on the accumulation and deposition of the comparable sized and processed fragments, it is likely that following a significant fracturing event on fresh bone, considerable rounding by abrasion occurred in fluvial transportation by fine-grained sands. The fragments were also exposed to some surface exposure taphonomy resulting in typical Stage 2 bone weathering. The combination of both surface weathering and fluvial transportation has resulted in the loss of much of the original surface of the bone fragments.

The mostly Whole Bone and Part Bone *Stegodon* material of Subset 2 was likely transported over relatively short distances compared to the many small bone fragments from Subset 1, based on the susceptibility of bones to fluvial transport described by Voorhies [48]. Voorhies foundation experiments used disarticulated coyote and sheep skeletons to measure characteristic susceptibility to transport; however, further experimentation by Frison and Todd (1986) [47] using bones of a modern elephant augmented proboscidean fluvial transportation susceptibility. The resultant Fluvial Transport Index (FTI) grouped elephant bones based on their transport potential: a high FTI corresponds with high transport potential and a low FTI with low transport potential with a range of 1–100. Frison and Todd (1986) observed similar patterns to those of Voorhies and aligned an FTI of greater than 75 with the Voorhies Group 1 (sacrum, patella, astragalus, calcaneus, all vertebrae excluding atlas), FTI 50–74 with Voorhies Group 2 (ribs, scapula, humerus, tibia, metacarpals), and FTI less than 50 with Voorhies Group 3 (cranium, mandible, atlas, pelvis, femur, radius, ulna) [47].

Subset 2 long limb bones, selected as representing a potential indicator of hominin food procurement, corresponding with Voorhies Group 2/3 and FTI ranging between 50–100, have potential transport characteristics of bones gradually or intermittently moving in periods of higher velocity river discharge while staying in contact with the bottom. The long limb bones were less rounded when compared with the Subset 1 material; however, some loss of surface features was observed, such as rounding on protruding muscle attachments, tuberosities, and epiphyseal ends. Rounding was likely caused during water flow, caused by the bone abrading with particles on the bottom of the channel, and as particles moved above the bone as it remained settled on the base of the channel.

## 5. Conclusions

The present taphonomic analysis of the Upper Fossil-bearing Interval at Mata Menge supports previous interpretations that the site represents a stream channel. The analysis further suggests that fluvial transport has affected the assemblage, causing significant obliteration of bone surface characteristics and rounding during fluvial transport. This is particularly noted in the small fragments of bone for which the original skeletal element could not be identified due to their small size but that were attributed to *Stegodon* based on cortical bone thickness. While the possibility of identifying additional hominin material in this assemblage is high, it is very unlikely that any remains would be found in articulation. The high density of small fragments of bone that have undergone significant modification by weathering, fragmentation, and fluvial abrasion do align with the characteristics of the existing hominin fossils found at the UFI at Mata Menge, and additional material would likely present these same characteristics. The taphonomic processes identified from this study would likely have a significant effect on the remains of the small-bodied hominin, *Homo floresiensis*, identified from this location. The resultant disarticulation, fragmentation, transportation, and bone surface modifications certainly remove the likelihood of locating a fully or partially articulated hominin skeleton.

Overall the two examined subsets reveal an observed consistency in the extent of weathering for the examined material, with most material exhibiting Stage 2 weathering. Some evidence for *Stegodon* trampling bone modifications were identified with differential weathering observed on the proximal and distal ends of two ulna bones. It appears that the material in each subset is the result of different taphonomic processing after the death of the animal, with Subset 1 material exposed to further fragmentation processing, while Subset 2 remained mostly intact. Approximately 10% of all material scored 3 or 4 on the FFI, characteristic of fracturing on fresh and unfresh bone; however, extensive rounding, weathering, and further dry bone fracturing has possibly obscured any initial fresh bone fracturing. Subset 1 material was consistently highly fragmented, with more than half being unidentifiable bone fragments <30 mm in length with rounded fractured edges likely abraded in significant fluvial transportation. This preliminary taphonomic analysis at Mata Menge has identified differential presentation of material here, indicating multiple taphonomic processing events contributing to the formation of this bonebed.

**Author Contributions:** Conceptualisation, M.J.P. and G.D.v.d.B.; methodology, M.J.P.; validation, M.J.P., G.D.v.d.B., and K.M.M.; formal analysis, M.J.P.; investigation, M.J.P.; resources, I.S. and U.P.W.; data curation, M.J.P.; writing—original draft preparation, M.J.P.; writing—review and editing, M.J.P. and G.D.v.d.B.; visualisation, M.J.P.; supervision, G.D.v.d.B.; project administration, G.D.v.d.B.; funding acquisition, G.D.v.d.B. All authors have read and agreed to the published version of the manuscript.

**Funding:** This research was funded by an Australian Research Council grant to Gert van den Bergh, grant number DP190100164. Tickets to Bandung were financed by a student support grant from the Faculty of Science, Medicine and Health (SMAH) of the University of Wollongong.

**Institutional Review Board Statement:** Not applicable.

**Informed Consent Statement:** Not applicable.

**Data Availability Statement:** The data presented in this study are available on request from the corresponding author. The data are not publicly available due to the university policy on delaying access to thesis and related data until post-publication.

**Acknowledgments:** The authors would like to sincerely thank the three anonymous reviewers for their careful comments, which greatly improved the manuscript. We would also like to thank the academic editors for their thoughtful comments during this process too. Additional logistic and in-kind support from the Geological Survey Institute (GSI) and the Museum Geologi Bandung, Indonesia. Thank you to Iwan Kurniawan, Director of the Geology Museum Bandung, for access to the fossil collections. Scientific and technical personnel involved during the fieldwork campaigns, including: Ruly Setiawan, Dida Yurnaldi, Erick Setiyabudi, Ifan Yoga Pertama, Susan Hayes, supported in the

field by 46 local people from the villages Mengeruda, Piga-I and Piga-II, and Fransiskus Bani and family for hospitality in Mengeruda.

**Conflicts of Interest:** The authors declare no conflict of interest.

## References

- Hooijer, D.A. A stegodon from flores. *Treubia* **1957**, *24*, 119–128.
- Verhoeven, T. Pleistozäne Funde in Flores. *Anthropos* **1958**, *53*, 264–265.
- Aziz, F.; Morwood, M.J. Introduction: geology, palaeontology and archaeology of the Soa Basin, Central Flores, Indonesia. In *Pleistocene Geology, Palaeontology and Archaeology of the Soa Basin, Central Flores, Indonesia*; Aziz, F., Morwood, M.J., van den Bergh, G.D., Eds.; Pusat Survei Geologi, Badan Geologi, Departemen Energi dan Sumber Daya Mineral: Bandung, Indonesia, 2009; pp. 1–18.
- van den Bergh, G.D.; Kurniawan, I.; Morwood, M.J.; Lentfer, C.J.; Suyono; Setiawan, R.; Aziz, F. Environmental reconstruction of the Middle Pleistocene archaeological/palaeontological site Mata Menge, Flores, Indonesia. In *Pleistocene Geology, Palaeontology and Archaeology of the Soa Basin, Central Flores, Indonesia*; Aziz, F., Morwood, M.J., van den Bergh, G.D., Eds.; Pusat Survei Geologi, Badan Geologi, Departemen Energi dan Sumber Daya Mineral: Bandung, Indonesia, 2009; pp. 59–94.
- van den Bergh, G.D.; Mubroto, B.; Aziz, F.; Sondaar, P.Y.; Vos, J. Did *Homo erectus* reach the Island of Flores? *Bull. Indo-Pac. Prehist. Assoc.* **1996**, *14*, 27–36. [[CrossRef](#)]
- van den Bergh, G.D. The Late Neogene Elephantoid-Bearing Faunas of Indonesia and Their Palaeozoogeographic Implications: A Study of the Terrestrial Faunal Succession of Sulawesi, Flores and Java, Including Evidence for Early Hominid Dispersal East of Wallace's Line. Ph.D. Thesis, University of Utrecht, Utrecht, The Netherlands, 1999.
- Sondaar, P.Y.; van den Bergh, G.D.; Mubroto, B.; Aziz, F.; de Vos, J.; Batu, U.L. Middle Pleistocene faunal turnover and colonization of Flores (Indonesia) by *Homo erectus*. *Comptes Rendus de l'Academie des Sciences de Paris* **1994**, *319*, 1255–1262.
- Brumm, A.; Aziz, F.; van den Bergh, G.D.; Morwood, M.J.; Moore, M.W.; Kurniawan, I.; Hobbs, D.R.; Fullagar, R. Early stone technology on Flores and its implications for *Homo floresiensis*. *Nature* **2006**, *441*, 624–628. [[CrossRef](#)]
- Brumm, A.; Jensen, G.M.; van den Bergh, G.D.; Morwood, M.J.; Kurniawan, I.; Aziz, F.; Storey, M. Hominins on Flores, Indonesia, by one million years ago. *Nature* **2010**, *464*, 748–752. [[CrossRef](#)]
- Brumm, A.; van den Bergh, G.D.; Storey, M.; Kurniawan, I.; Alloway, B.V.; Setiawan, R.; Setiyabudi, E.; Gruen, R.; Moore, M.W.; Yurnaldi, D.; et al. Age and context of the oldest known hominin fossils from Flores. *Nature* **2016**, *534*, 249. [[CrossRef](#)]
- Morwood, M.J.; Aziz, F.; van den Bergh, G.D.; Sondaar, P.Y.; De Vos, J. Stone Artefacts from the 1994 Excavation at Mata Menge, West Central Flores, Indonesia. *Aust. Archaeol.* **1997**, *44*, 26–34. [[CrossRef](#)]
- Morwood, M.J.; O'Sullivan, P.B.; Aziz, F.; Raza, A. Fission-track ages of stone tools and fossils on the east Indonesian Island of Flores. *Nature* **1998**, *392*, 173–176. [[CrossRef](#)]
- O'Sullivan, P.B.; Morwood, M.J.; Hobbs, D.; Aziz Suminto, F.; Situmorang, M.; Raza, A.; Maas, R. Archaeological implications of the geology and chronology of the Soa basin, Flores, Indonesia. *Geology* **2001**, *29*, 607. [[CrossRef](#)]
- van den Bergh, G.D.; Kaifu, Y.; Kurniawan, I.; Kono, R.T.; Brumm, A.; Setiyabudi, E.; Aziz, F.; Morwood, M.J. *Homo floresiensis*-like fossils from the early middle Pleistocene of Flores. *Nature* **2016**, *534*, 245–248. [[CrossRef](#)]
- Yurnaldi, D.; Setiawan, R.; Patriani, E. The Magnetostratigraphy and the Age of So'a Basin Fossil-Bearing Sequence, Flores, Indonesia. *Indones. J. Geosci.* **2018**, *5*. [[CrossRef](#)]
- Sutikna, T.; Tocheri, M.W.; Morwood, M.J.; Saptomo, E.W.; Jatmiko; Awe, R.D.; Wasisto, S.; Westaway, K.E.; Aubert, M.; Li, B.; et al. Revised stratigraphy and chronology for *Homo floresiensis* at Liang Bua in Indonesia. *Nature* **2016**, *532*, 366–369. [[CrossRef](#)]
- Meijer, H.J.M.; D'Errico, F.; Queffelec, A.; Kurniawan, I.; Setiyabudi, E.; Sutisna, I.; Brumm, A.; van den Bergh, G.D. Characterization of bone surface modifications on an early to middle Pleistocene bird assemblage from Mata Menge (Flores, Indonesia) using multifocus and confocal microscopy. *Palaeogeogr. Palaeoclimatol. Palaeoecol.* **2019**, *529*, 1–11. [[CrossRef](#)]
- Meijer, H.J.M.; Kurniawan, I.; Setiyabudi, E.; Brumm, A.; Sutikna, T.; Setiawan, R.; van den Bergh, G.D. Avian remains from the early/middle Pleistocene of the So'a Basin, central Flores, Indonesia, and their palaeoenvironmental significance. *Palaeogeogr. Palaeoclimatol. Palaeoecol.* **2015**, *440*, 161–171. [[CrossRef](#)]
- Ali, J.R.; Heaney, L.R. Wallace's line, Wallacea, and associated divides and areas: history of a tortuous tangle of ideas and labels. *Biol. Rev.* **2021**. [[CrossRef](#)]
- Suminto; Morwood, M.J.; Kurniawan, I.; Aziz, F.; van den Bergh, G.D.; Hobbs, D.R. Geology and fossil sites of the Soa Basin, Flores, Indonesia. In *Pleistocene Geology, Palaeontology and Archaeology of the Soa Basin, Central Flores, Indonesia*; Aziz, F., Morwood, M.J., van de Bergh, G.D., Eds.; Pusat Survei Geologi, Badan Geologi, Departemen Energi dan Sumber Daya Mineral: Bandung, Indonesia, 2009; pp. 19–40.
- Aziz, F.; van den Bergh, G.D.; Morwood, M.J.; Hobbs, D.R.; Kurniawan, I.; Collins, J.; Jatmiko. Excavations at Tangi Talo, central Flores, Indonesia. In *Pleistocene Geology, Palaeontology and Archaeology of the Soa Basin, Central Flores, Indonesia*; Aziz, F., Morwood, M.J., van den Bergh, G.D., Eds.; Pusat Survei Geologi, Badan Geologi, Departemen Energi dan Sumber Daya Mineral: Bandung, Indonesia, 2009; pp. 41–58.
- Sondaar, P.Y. Faunal evolution and the mammalian biostratigraphy of Java. *Cour. Forsch. Inst. Senckenberg* **1984**, *69*, 219–235.
- Morwood, M.J.; Aziz, F.; O'Sullivan, P.; Nasruddin; Hobbs, D.R.; Raza, A. Archaeological and palaeontological research in central Flores, east Indonesia: Results of fieldwork 1997–98. *Antiquity* **1999**, *73*, 273–286. [[CrossRef](#)]

24. van den Bergh, G.D.; de Vos, J.; Sondaar, P.Y. The late Quaternary palaeogeography of mammal evolution in the Indonesian Archipelago. *Palaeogeogr. Palaeoclimatol. Palaeoecol.* **2001**, *171*, 385–408. [[CrossRef](#)]
25. van den Bergh, G.D.; Awe, R.D.; Morwood, M.J.; Sutikna, T.; Jatmiko; Wahyu Saptomo, E. The youngest stegodon remains in Southeast Asia from the Late Pleistocene archaeological site Liang Bua, Flores, Indonesia. *Quat. Int.* **2008**, *182*, 16–48. [[CrossRef](#)]
26. van den Bergh, G.D. *Insular Fossil Fauna through Deep Geological Time of Wallacea*; Geological Survey Center Indonesia, University of Wollongong Australia: Wollongong, NSW, Australia, 2019.
27. Faith, J.T.; Behrensmeyer, A.K. Changing patterns of carnivore modification in a landscape bone assemblage, Amboseli Park, Kenya. *J. Archaeol. Sci.* **2006**, *33*, 1718–1733. [[CrossRef](#)]
28. Haynes, G. Longitudinal studies of African elephant death and bone deposits. *J. Archaeol. Sci.* **1988**, *15*, 131–157. [[CrossRef](#)]
29. Haynes, G. Mammoth landscapes: Good country for hunter-gatherers. *Quat. Int.* **2006**, *142*, 20–29. [[CrossRef](#)]
30. Haynes, G.; Krasinski, K. Taphonomic Fieldwork in Southern Africa and its Application in Studies of the Earliest Peopling of North America. *J. Taphon.* **2010**, *8*, 181–202.
31. D'Amore, D.C.; Blumenschine, R.J. Komodo monitor (*Varanus komodoensis*) feeding behaviour and dental function reflected through tooth marks on bone surfaces and the application to ziphodont paleobiology. *Paleobiology* **2009**, *35*, 525–552. [[CrossRef](#)]
32. Njau, J.K.; Blumenschine, R.J. A diagnosis of crocodile feeding traces on larger mammal bone, with fossil examples from the Plio-Pleistocene Olduvai Basin, Tanzania. *J. Hum. Evol.* **2006**, *50*, 142–162. [[CrossRef](#)]
33. Sahle, Y.; Zaatari Sireen, E.; White Tim, D. Hominid butchers and biting crocodiles in the African Plio-Pleistocene. *Proc. Natl. Acad. Sci. USA* **2017**, *114*, 13164. [[CrossRef](#)]
34. Domínguez-Rodrigo, M.; Baquedano, E. Distinguishing butchery cut marks from crocodile bite marks through machine learning methods. *Sci. Rep.* **2018**, *8*. [[CrossRef](#)]
35. van den Bergh, G.D.; Meijer, H.J.M.; Due Awe, R.; Morwood, M.J.; Szabo, K.A.; van den Hoek Ostenda, L.W.; Sutikna, T.; Saptomo, E.W.; Piper, P.J.; Dobney, K.M. The Liang Bua faunal remains: a 95 k.yr. sequence from Flores, East Indonesia. *J. Hum. Evol.* **2009**, *57*, 527–537. [[CrossRef](#)]
36. Badgley, C. Counting individuals in mammalian fossil assemblages from fluvial environments. *PALAIOS* **1986**, *1*, 328–338. [[CrossRef](#)]
37. Brumm, A.; Moore, M.W.; van den Bergh, G.D.; Kurniawan, I.; Morwood, M.J.; Aziz, F. Stone technology at the Middle Pleistocene site of Mata Menge, Flores, Indonesia. *J. Archaeol. Sci.* **2010**, *37*, 451–473. [[CrossRef](#)]
38. Dennell, R.W.; Coard, R.; Turner, A. Predators and scavengers in Early Pleistocene southern Asia. *Quat. Int.* **2008**, *192*, 78–88. [[CrossRef](#)]
39. Lyman, R.L. Archaeofaunas and Butchery Studies: A Taphonomic Perspective. *Adv. Archaeol. Method Theory* **1987**, *10*, 249–337.
40. Arroyo-Cabrales, J.; Johnson, E.; Morett, L. Mammoth bone technology in the Basin of Mexico. In *Bones for Tools—Tools for Bones: the Interplay Between Objects and Objectives*; Seetah, K., Gravina, B., Eds.; McDonald Institute for Archaeological Research: Cambridge, UK, 2012; pp. 97–113.
41. Morlan, R.E. Toward the definition of criteria for the recognition of artificial bone alterations. *Quat. Res.* **1984**, *22*, 160–171. [[CrossRef](#)]
42. Villa, P.; Mahieu, E. Breakage patterns of human long bones. *J. Hum. Evol.* **1991**, *21*, 27–48. [[CrossRef](#)]
43. Fernandez-Jalvo, Y.; Andrews, P.; Denys, C.; Sese, C.; Stoetzel, E.; Marin-Monfort, D.; Pesquero, D. Taphonomy for taxonomists; implications of predation in small mammal studies. *Quat. Sci. Rev.* **2016**, *139*, 138–157. [[CrossRef](#)]
44. Prasanth, T.; Saraswathi, T.R. Histopathological and radiographic evaluation of rat molar teeth after traumatic injury—A pilot study. *J. Oral Maxillofac. Pathol.* **2012**, *16*, 313–317. [[CrossRef](#)]
45. Haynes, G.; Krasinski, K.; Wojtal, P. Elephant bone breakage and surface marks made by trampling elephants: Implications for interpretations of marked and broken *Mammuthus* spp. bones. *J. Archaeol. Sci. Rep.* **2020**, *33*, 102491. [[CrossRef](#)]
46. Behrensmeyer, A.K. Vertebrate preservation in fluvial channels. *Palaeogr. Palaeoclimatol. Palaeoecol.* **1988**, *63*, 188–199. [[CrossRef](#)]
47. Frison, G.C.; Todd, L.C. *The Colby Mammoth Site: Taphonomy and Archeology of a Clovis Kill in Northern Wyoming*; University of New Mexico Press: Albuquerque, NM, USA, 1986.
48. Voorhies, M. *Taphonomy and Population Dynamics of an Early Pliocene Vertebrate Fauna, Knox County, Nebraska*; University of Wyoming: Laramie, WY, USA, 1969.
49. Behrensmeyer, A.K. The Taphonomy and Paleocology of Plio-Pleistocene Vertebrate Assemblages East of Lake Rudolf, Kenya. *Bull. Museum Comp. Zool.* **1975**, *146*, 473–578.
50. Coard, R. One bone, two bones, wet bones, dry bones: Transport potential under experimental conditions. *J. Archaeol. Sci.* **1999**, *26*, 1369–1375. [[CrossRef](#)]
51. Coard, R.; Dennell, R.W. Taphonomy of some articulated skeletal remains: Transport potential in an artificial environment. *J. Archaeol. Sci.* **1995**, *22*, 441–448. [[CrossRef](#)]
52. Pante, M.C.; Blumenschine, R.J. Fluvial transport of bovid long bones fragmented by the feeding activities of hominin and carnivore. *J. Archaeol. Sci.* **2010**, *37*, 846–854. [[CrossRef](#)]
53. Hjølström, F. Studies of the morphological activity of rivers as illustrated by the River Fyris. *Bull. Geol. Inst. Univ. Uppsala* **1935**, *25*, 221–527.
54. Behrensmeyer, A.K. Taphonomic and Ecological Information from Bone Weathering. *Paleobiology* **1978**, *4*, 150–162. [[CrossRef](#)]

55. Behrensmeier, A.K.; Miller, J.H. Building links between ecology and paleontology using taphonomic studies of recent vertebrate communities. In *Paleontology in Ecology and Conservation*; Louys, J., Ed.; Springer: Berlin/Heidelberg, Germany, 2012; pp. 69–91.
56. Lyman, R.L.; Fox, G.L. A critical evaluation of bone weathering as an indication of bone assemblage formation. *J. Archaeol. Sci.* **1989**, *16*, 293–317. [[CrossRef](#)]
57. Boschian, G.; Caramella, D.; Saccà, D.; Barkai, R. Are there marrow cavities in Pleistocene elephant limb bones, and was marrow available to early humans? New CT scan results from the site of Castel di Guido (Italy). *Quat. Sci. Rev.* **2019**, *215*, 86–97. [[CrossRef](#)]
58. Outram, A.K. The Identification and Palaeoeconomic Context of Prehistoric Bone Marrow and Grease Exploitation. Ph.D. Thesis, Thesis, University of Durham, Durham, UK, 1998.
59. Outram, A.K. A new approach to identifying bone marrow and grease exploitation: Why the “Indeterminate” fragments should not be ignored. *J. Archaeol. Sci.* **2001**, *28*, 401–410. [[CrossRef](#)]
60. Yravedra, J.; Panera, J.; Rubio-Jara, S.; Manzano, I.; Expósito, A.; Pérez-González, A.; Soto, E.; López-Recio, M. Neanderthal and *Mammuthus* interactions at EDAR Culebro 1 (Madrid, Spain). *J. Archaeol. Sci.* **2014**, *42*, 500–508. [[CrossRef](#)]
61. Yravedra, J.; Rubio-Jara, S.; Panera, J.; Uribealrrea, D.; Pérez-González, A. Elephants and subsistence. Evidence of the human exploitation of extremely large mammal bones from the Middle Palaeolithic site of PRERESA (Madrid, Spain). *J. Archaeol. Sci.* **2012**, *39*, 1063–1071. [[CrossRef](#)]
62. Yravedra, J.; Domínguez-Rodrigo, M.; Santonja, M.; Pérez-González, A.; Panera, J.; Rubio-Jara, S.; Baquedano, E. Cut marks on the Middle Pleistocene elephant carcass of Áridos 2 (Madrid, Spain). *J. Archaeol. Sci.* **2010**, *37*, 2469–2476. [[CrossRef](#)]
63. Company, J.; Pereda-Suberbiola, X. Long bone histology of a eusuchian crocodyliform from the Upper Cretaceous of Spain: Implications for growth strategy in extinct crocodiles. *Cretac.s Res.* **2017**, *72*, 1–7. [[CrossRef](#)]
64. Albéric, M.; Dean, M.N.; Gourrier, A.; Wagermaier, W.; Dunlop, J.W.C.; Staude, A.; Fratzl, P.; Reiche, I. Relation between the Macroscopic Pattern of Elephant Ivory and Its Three-Dimensional Micro-Tubular Network. *PLoS ONE* **2017**, *12*, e0166671. [[CrossRef](#)] [[PubMed](#)]
65. Outram, A.K. Bone Fracture and within-bone nutrients: an experimentally based method for investigating levels of marrow extraction. In *Consuming Passions and Patterns of Consumption*; Scarre, C., Ed.; McDonald Institute for Archaeology: Cambridge, UK, 2002; pp. 51–63.
66. Boyd, D.K.; Kenmotsu, N.A. *The Toyah Phase of Central Texas Late Prehistoric Economic and Social Processes*, 1st ed.; Texas A&M University Press: College Station, TX, USA, 2012.
67. Haynes, G.; Krasinski, K.; Wojtal, P. A Study of Fractured Proboscidean Bones in Recent and Fossil Assemblages. *J. Archaeol. Method Theory* **2020**. [[CrossRef](#)]
68. Johnson, E.V.; Parmenter, P.C.R.; Outram, A.K. A new approach to profiling taphonomic history through bone fracture analysis, with an example application to the Linearbandkeramik site of Ludwinowo 7. *J. Archaeol. Sci. Rep.* **2016**, *9*, 623–629. [[CrossRef](#)]
69. Karr, L.; Outram, A.; Hannus, L. A Chronology of Bone Marrow and Bone Grease Exploitation at the Mitchell Prehistoric Indian Village. *Plains Anthropol.* **2010**, *55*, 215–223. [[CrossRef](#)]
70. Karr, L.P. Brewster site zooarchaeology reinterpreted: understanding levels of animal exploitation and bone fat production at the Initial Middle Missouri type site. *STAR Sci. Technol. Archaeol. Res.* **2015**, *1*, 1–13. [[CrossRef](#)]
71. Outram, A. Distinguishing bone fat exploitation from other taphonomic processes: what caused the high level of bone fragmentation at the Middle Neolithic site of Ajvide, Gotland? In *The Zooarchaeology of Fats, Oils, Milk and Dairying. Proceedings of the 9th ICAZ Conference*; Oxbow Books: Oxford, UK, 2005.
72. Holen, S.R. Taphonomy of two last glacial maximum mammoth sites in the central Great Plains of North America: A preliminary report on La Sena and Lovewell. *Quat. Int.* **2006**, *142–143*, 30–43. [[CrossRef](#)]
73. van der Geer, A.A.E.; van den Bergh, G.D.; Lyras, G.A.; Prasetyo, U.W.; Due, R.A.; Setiyabudi, E.; Drinia, H. The effect of area and isolation on insular dwarf proboscideans. *J. Biogeogr.* **2016**, *43*, 1656–1666. [[CrossRef](#)]
74. Behrensmeier, A.K. Patterns of natural bone distribution on recent land surfaces: implications for archaeological site formation. In *Animals and Archaeology: 1. Hunters and Their Prey*; Clutton, B., Grigson, C., Eds.; British Archaeological Reports International Series; British Archaeological: Oxford, UK, 1983; Volume 163.
75. Lyman, R.L. *Vertebrate Taphonomy*; Cambridge University Press: Cambridge, UK, 1994.
76. Thompson, C.E.L.; Ball, S.; Thompson, T.J.U.; Gowland, R. The abrasion of modern and archaeological bones by mobile sediments: the importance of transport modes. *J. Archaeol. Sci.* **2011**, *38*, 784–793. [[CrossRef](#)]
77. Fernandez-Jalvo, Y.; Andrews, P. Experimental effects of water abrasion on bone fragments. *J. Taphon.* **2003**, *1*, 147–163.